

Suppressing Chromium Disproportion Reaction in O3-type Layered Cathode Material for High Capacity Sodium-ion Batteries

Ming-Hui Cao,^a Yong Wang,^c Zulipiya Shadike,^a Ji-Li Yue,^a Enyuan Hu,^d Seong-Min Bak,^d Yong-Ning Zhou*^b and Xiao-Qing Yang*^d and Zheng-Wen Fu*^a

^aShanghai Key Laboratory of Molecular Catalysts and Innovative Materials, Department of Chemistry & Laser Chemistry Institute, Fudan University, Shanghai, 200433, P.R. China *E-mail: zwfu@fudan.edu.cn

^bDepartment of Materials Science, Fudan University, Shanghai, 200433, P.R. China *E-mail: zhouyongning@gmail.com

^cShanghai Institute of Space Power-Sources, Shanghai, 200245, P.R. China.

^dDepartment of Chemistry, Brookhaven National Laboratory, Upton, New York 11973, USA *E-mail: xyang@bnl.gov

Electronic Supplementary Information (ESI)

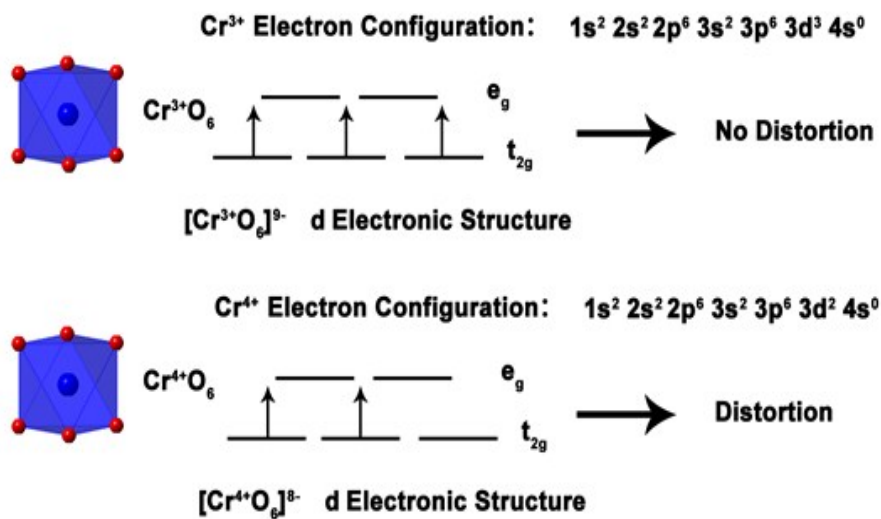


Figure S1. Electron configuration and distortion schematics of Cr³⁺ and Cr⁴⁺ in CrO₆ octahedral coordination. ^[S1]

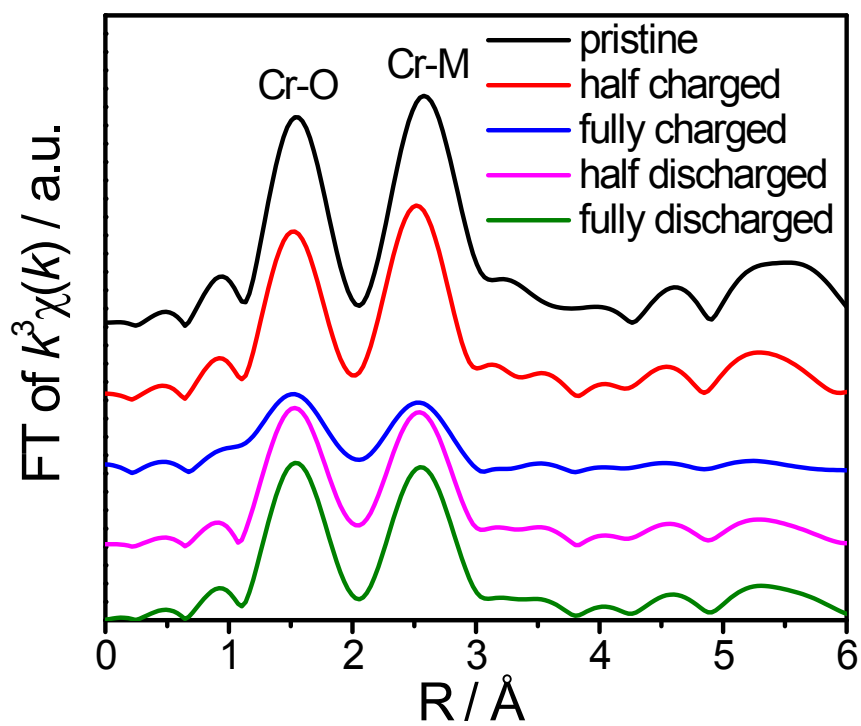


Figure S2. Fourier transform X-ray absorption near-edge structure (XANES) spectra at Cr K-edges of NCFM electrodes during the initial cycle.

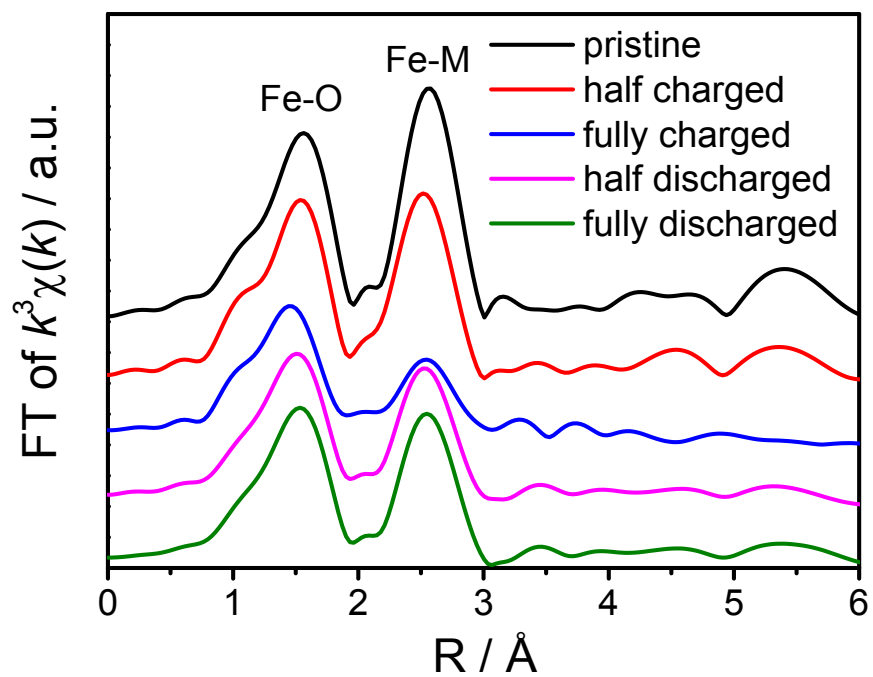


Figure S3. Fourier transform X-ray absorption near-edge structure (XANES) spectra at Fe K-edges of NCFM electrodes during the initial cycle.

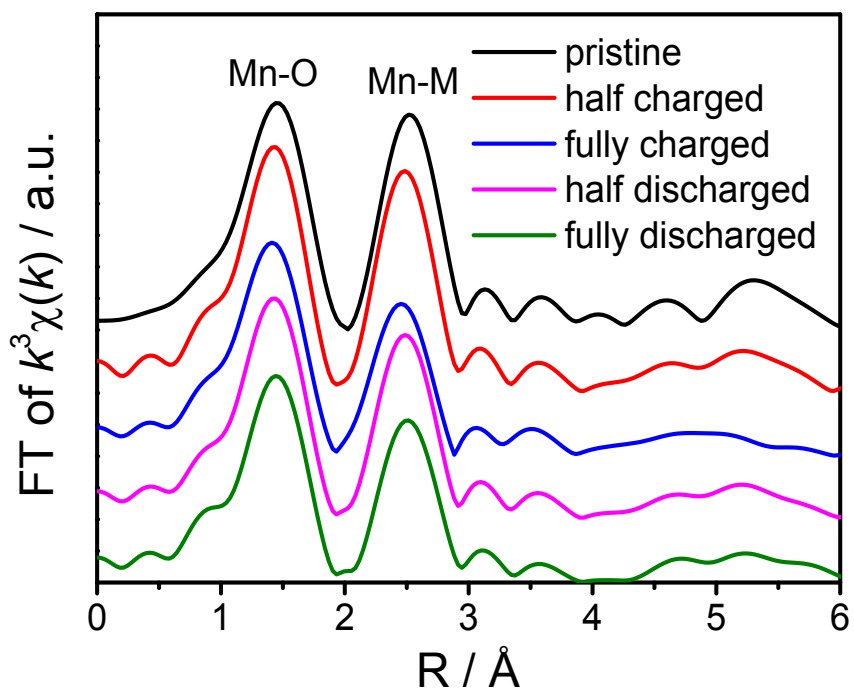


Figure S4. Fourier transform X-ray absorption near-edge structure (XANES) spectra at Mn K-edges of NCFM electrodes during the initial cycle.

Table S1. Structural parameters and atomic positions of as-prepared O3-type $\text{NaCr}_{1/3}\text{Fe}_{1/3}\text{Mn}_{1/3}\text{O}_2$ deduced from Rietveld Refinement.

<i>Atom</i>	<i>Wyckoff</i>	<i>Occupancy</i>	<i>x/a</i>	<i>y/b</i>	<i>z/c</i>
<i>Na</i>	3b	1	0	0	0.0
<i>Cr</i>	3a	1/3	0	0	0.5
<i>Fe</i>	3a	1/3	0	0	0.5
<i>Mn</i>	3a	1/3	0	0	0.5
<i>O</i>	6c	1	0	0	0.230065
R-3m:	$a = b = 2.9639(4) \text{ \AA}$		$c = 16.1693(5) \text{ \AA}$		
	$R_p = 1.91\%$	$R_{wp} = 2.9\%$	$GOF(\chi^2) = 1.102$		

Table S2. Comparison of the electrochemical properties of O3-layered cathode materials for sodium ion batteries.

	Electrode materials	Voltage Range (V)	Initial Capacity (mAh/g)	Reference
unary	NaNiO ₂	1.25-3.75	125(0.1C)	S2
	NaFeO ₂	1.5-3.6	82(0.1C)	S3
	NaTiO ₂	0.6-1.6	152(0.1C)	S4
	NaCoO ₂	2.0-3.8	116(0.1C)	S5
	α-NaMnO ₂	2.0-3.8	187(0.1C)	S6
	β-NaMnO ₂	2.0-4.2	No Info.	S7
	NaCrO ₂	2.0-3.6	112(0.1C)	S8
	NaCrO ₂ /C	2.0-3.6	121(0.1C)	S8
Binary	NaNi _{0.5} Mn _{0.5} O ₂	2.2-3.8	125(0.033C)	S9
	NaFe _{0.5} Co _{0.5} O ₂	2.5-4.0	160(0.1C)	S10
	NaNi _{0.5} Ti _{0.5} O ₂	2.0-4.0	102(0.1C)	S11
	NaMn _{0.5} Fe _{0.5} O ₂	1.5-4.2	135(0.01C)	S12
	NaFe _{0.5} Mn _{0.5} O ₂	1.5-4.2	125(0.05C)	S13
Ternary	NaNi _{0.25} Fe _{0.5} Mn _{0.25} O ₂	2.1-3.9	140(0.1C)	S14
	NaNi _{0.33} Mn _{0.33} Co _{0.33} O ₂	2.0-3.75	120(0.1C)	S15
	NaNi _{0.33} Fe _{0.33} Mn _{0.33} O ₂	2.0-4.0	125(0.1C)	S16
	NaNi _{0.4} Fe _{0.2} Mn _{0.4} O ₂	2.0-4.0	131(0.1C)	S17
	NaNi _{0.33} Co _{0.33} Fe _{0.33} O ₂	2.0-4.2	165(0.1C)	S18
	NaFe _{0.2} Ni _{0.4} Ti _{0.4} O ₂	2.6-3.75	120(0.1C)	S19
	NaFe _{0.2} (Ni _{1/2} Ti _{1/2}) _{0.6} O ₂	2.0-3.8	130(0.05C)	S20
	NaFe_{0.33}Cr_{0.33}Mn_{0.33}O₂	1.5-4.2	186(0.05C)	This work
Quaternary	NaNi _{0.25} Fe _{0.25} Co _{0.25} Mn _{0.25} O ₂	1.9-4.3	183(0.1C)	S21
	NaNi _{0.4} Fe _{0.2} Mn _{0.25} Ti _{0.2} O ₂	2.0-4.2	145(0.1C)	S22
Quinary	NaNi _{0.25} Fe _{0.25} Co _{0.25} Mn _{0.125} Ti _{0.125} O ₂	2.0-4.1	128(0.1C)	S23

Tables S3. Structure parameters from nonlinear least-squares fits to the first two peaks of the Fourier transform at the Cr K-edge EXAFS of NCFM electrode at different states.

Samples	Path	$r/\text{\AA}$	$\sigma^2 / 10^{-3}\text{\AA}^2$	$\Delta E/\text{eV}$	R
pristine	Cr-O	1.99(1) \pm 0.013	0.10 \pm 2.10	0.95 \pm 1.78	0.011
	Cr-TM	2.95(9) \pm 0.014	1.10 \pm 1.77		
half charged	Cr-O	1.95(6) \pm 0.017	2.20 \pm 2.84	-1.36 \pm 2.32	0.018
	Cr-TM	2.92(7) \pm 0.018	2.84 \pm 2.33		
fully charged	Cr-O	1.97(3) \pm 0.029	3.13 \pm 1.86	-2.67 \pm 2.18	0.005
	Cr-TM	2.93(3) \pm 0.037	4.26 \pm 1.47		
half discharged	Cr-O	1.97(8) \pm 0.016	0.14 \pm 2.66	-1.19 \pm 2.41	0.019
	Cr-TM	2.94(6) \pm 0.019	2.33 \pm 2.44		
fully discharged	Cr-O	1.98(3) \pm 0.016	0.37 \pm 2.41	0.55 \pm 2.30	0.002
	Cr-TM	2.95(9) \pm 0.018	2.64 \pm 2.36		

r : bond length; σ^2 : Debye-Waller factor (disorder); ΔE : inner shell potential shift; R : R-factor.

Table S4. Structure parameters from nonlinear least-squares fits to the first two peaks of the Fourier transform at the Fe K-edge EXAFS of NCFM electrode at different states.

Samples	Path	$r/\text{\AA}$	$\sigma^2 / 10^{-3}\text{\AA}^2$	$\Delta E/\text{eV}$	R
pristine	Mn-O	1.90(8) \pm 0.008	2.55 \pm 1.25	-4.38 \pm 1.20	0.006
	Mn-TM	2.94(9) \pm 0.009	3.90 \pm 1.05		
half charged	Mn-O	1.90(2) \pm 0.010	2.78 \pm 1.59	-4.74 \pm 1.51	0.010
	Mn-TM	2.93(2) \pm 0.011	4.10 \pm 1.34		
fully charged	Mn-O	1.89(4) \pm 0.014	7.79 \pm 1.84	-5.09 \pm 1.80	0.013
	Mn-TM	2.91(9) \pm 0.011	3.75 \pm 2.55		
half discharged	Mn-O	1.90(2) \pm 0.009	2.88 \pm 1.48	-4.82 \pm 1.44	0.009
	Mn-TM	2.93(8) \pm 0.011	5.07 \pm 1.32		
fully discharged	Mn-O	1.91(2) \pm 0.009	2.25 \pm 1.53	-3.57 \pm 1.52	0.010
	Mn-TM	2.95(7) \pm 0.012	4.92 \pm 1.41		

r : bond length; σ^2 : Debye-Waller factor (disorder); ΔE : inner shell potential shift; R : R-factor.

Table S5. Structure parameters from nonlinear least-squares fits to the first two peaks of the Fourier transform at the Mn K-edge EXAFS of NCFM electrode at different states.

Samples	Path	$r/\text{\AA}$	$\sigma^2 / 10^{-3}\text{\AA}^2$	$\Delta E/\text{eV}$	R
pristine	Fe-O	2.03(1) \pm 0.006	4.72 \pm 0.90	-0.83 \pm 0.61	0.002
	Fe-TM	2.98(2) \pm 0.005	4.21 \pm 0.65		
half charged	Fe-O	2.01(4) \pm 0.005	6.58 \pm 0.85	-1.23 \pm 0.55	0.002
	Fe-TM	2.96(8) \pm 0.005	6.62 \pm 0.64		
fully charged	Fe-O	1.96(6) \pm 0.014	8.43 \pm 2.40	-1.40 \pm 1.73	0.013
	Fe-TM	2.98(0) \pm 0.020	14.01 \pm 2.55		
half discharged	Fe-O	2.00(0) \pm 0.007	7.20 \pm 1.19	-1.34 \pm 0.79	0.003
	Fe-TM	2.98(4) \pm 0.008	8.54 \pm 0.97		
fully discharged	Fe-O	2.01(5) \pm 0.006	6.32 \pm 1.09	-0.95 \pm 0.73	0.003
	Fe-TM	2.99(5) \pm 0.007	7.08 \pm 0.86		

r : bond length; σ^2 : Debye-Waller factor (disorder); ΔE : inner shell potential shift; R : R-factor.

Tables S6. Electronegativity parameters of ions in NCFM. [S24]

ions	Z*	r/Å	X _i
Fe ³⁺	4.95	1.24	1.9
Cr ⁴⁺	5.5	1.85	3.917
Mn ⁴⁺	5.65	1.79	4.09
Z*:effective nuclear number	r:atomic radius;	X _i :electronegativity	

$$X_{\text{Fe}^{3+}} < X_{\text{Cr}^{4+}} < X_{\text{Mn}^{4+}}$$

Electronic Configuration of Ions: 1s²2s²2p⁶3s²3p⁶3d^y4s⁰

Correlation Formula:

$$Z^* = Z - [0 \times 0.35 + (8+y) \times 0.85 + 10 \times 1.0]$$

$$3.59 \times 10^3 \times Z^* \text{ (pm)}^2$$

$$X_i = \frac{r^2}{Z^*} + 0.744$$

References

- [S1] T.P. Zhang., Journal of Higher Correspondence Education (Natural Sciences). 2003, **16**,31.
- [S2] X. H. Ma, H. L. Chen and G. Ceder, *J. Electrochem. Soc.* 2011, **158**, A1307.
- [S3] N. Yabuuchi, H. Yoshida and S. Komaba, *Electrochemistry* 2012, **80**, 716.
- [S4] D. Wu, X. Li, B. Xu, N. Twu, L. Liu and G. Ceder. *Energy Environ. Sci.* 2015, **8**, 195.
- [S5] T. Shibata, Y. Fukuzumi, W. Kobayashi and Yutaka Moritomo, *Sci. Rep.* 2015, **5**, 9006.
- [S6] X. H. Ma, H. L. Chen and G. Ceder, *J. Electrochem. Soc.* 2011, **158**, A1307.
- [S7] J. Billaud, R. J. Clement, A. R. Armstrong, J. Canales-Vazquez, P. Rozier, C. P. Grey and P. G. Bruce, *J. Am. Chem. Soc.* 2014, **136**, 17243.
- [S8] C. Y. Yu, J. S. Park, H. G. Jung, K. Y. Chung, D. Aurbach, Y. K. Sun and S. T. Myung, *Energy Environ. Sci.* 2015, **8**, 2019-2026
- [S9] S. Komaba, N. Yabuuchi, T. Nakayama, A. Ogata, T. Ishikawa and I. Nakai, *Inorg. Chem.* 2012, **51**,6211.
- [S10] H. Yoshida, N. Yabuuchi and S. Komaba, *Electrochem. Commun.* 2013, **34**, 60.
- [S11] H. J. Yu, S. H. Guo, Y. B. Zhu, M. Ishida and H. S. Zhou, *Chem. Commun.* 2014, **50**, 457.
- [S12] B. Mortemard de Boisse, D. Carlier, M. Guignard and C. Delmas, *J. Electrochem. Soc.* 2013, **160**, A569.
- [S13] N. Yabuuchi, M. Kajiyama, J. Iwatat, H. Nishikawa, S. Hitomi, R. Okuyama, R. Usui, Y. Yamada, S. Komaba, *Nat. Mater.* 2012, **11**, 512.
- [S14] S. M. Oh, S. T. Myung, C. S. Yoon, J. Lu, J. Hassoun, B. Scrosati, K. Amine and Y. K. Sun, *NanoLett.* 2014, **4**, 1620.
- [S15] M. Sathiya, K. Hemalatha, K. Ramesha, J.-M. Tarascon and A. S. Prakash, *Chem. Mater.*, 2012, **24**,1846.
- [S16] D. Kim, E. Lee, M. Slater, W. Lu, S. Rood and C.S. Johnson, *Electrochem. Commun.* 2012, **18**, 66.
- [S17] D. D. Yuan, Y. X. Wang, Y. L. Cao, X. P. Ai and H. X. Yang, *ACS Appl. Mater. Interfaces*, 2015, **7**, 8585.
- [S18] P. Vassilaras, A. J. Toumar and G. Ceder, *Electrochem. Commun.* 2014, **38**, 79.
- [S19] G. Singh, F. Aguesse, L. Otaegui, E. Goikolea, E. Gonzalo, J Segalini and T. Rojo. *J. Power Sources* 2015, **273**, 333.
- [S20] N. Yabuuchi, M. Yano, H. Yoshida, S. Kuze and S. Komaba, *J. Electrochem. Soc.* 2013, **160**, A3131.
- [S21] X. Li, D. Wu, Y. N. Zhou, L. Liu, X. Q. Yang and G. Ceder, *Electrochem. Commun.* 2014, **49**, 51.
- [S22] X. Sun, Y. Jin, C. Y. Zhang, J. W. Wen, Y. Shao, Y. Zang and C. H. Chen, *J. Mater. Chem. A* 2014, **2**, 17268.
- [S23] J. L. Yue, W. W. Yin, M. H. Cao, S. Zulipiya, Y. N. Zhou and Z.W. Fu, *Chem. Comm.* 2015 **51**, 15712.
- [S24] X. H. Yuan, Y. Li, Guangzhou Chemical Industry 2002, **30**, 134.